Structure-function relationships in human salivary α-amylase: role of aromatic residues

Narayanan RAMASUBBU[1]*, Chandran RAGUNATH[1], Krishnan SUNDAR[1], Prasunkumar J. MISHRA[1], Gyöngyi GYÉMÁNT[2] & Lili KANDRA[2]

[1]*Department of Oral Biology, University of Medicine and Dentistry of New Jersey, Newark, NJ 07103 USA; phone: ++ 1 973 972 0704, fax: ++ 1 973 972 0045, e-mail: n.ramasubbu@umdnj.edu*

[2]*Department of Biochemistry, Faculty of Sciences, University of Debrecen, P. O. Box 55, H-4010 Debrecen, Hungary*

Abstract: The active site of human salivary α-amylase consists of six subsites (-4 through $+2$). The aromatic residues, Trp58, Trp59, Tyr151 and Phe256 are prominently located at the active site (immediately next to the subsites -1 and $+1$ where cleavage occurs). We focused on determining the role of these aromatic residues in the structure-function relationships of salivary α-amylase. While previous studies had showed that glucose production was significant when residues Trp58 and Trp59 were mutated, results presented here show that at low concentrations of substrates, glucose production by Trp58 mutants was even higher. Unlike the wild-type enzyme, these Trp mutants acquired the ability to hydrolyze maltose and maltotriose, suggesting that impaired binding at subsites -2 and -3 might have increased the productive binding modes for the smaller oligosaccharides. The increase in transglycosylation activity by the mutant Y151M was further studied by analyzing the crystal structure of a complex between acarbose and Y151M. The mutant Y151M also modified acarbose in the crystal; however, only glucose.acarviosine was fitted at the active site (subsites -2, -1, $+1$). The aromatic residues, Phe256 and Phe295 prominent at the chloride-binding site (about 5Å away from the subsites -1 and $+1$) did not exhibit any significant effect in chloride binding; however, Phe256 helps orient a water chain that may be involved in the starch hydrolysis. From these studies, we conclude that aromatic residues in the vicinity of the active site of human salivary α-amylase play a crucial role in substrate binding, enzyme activity and catalysis.

Key words: salivary α-amylase, site-directed mutagenesis, subsite engineering, oligosaccharide hydrolysis, crystal structure.

Abbreviations: CNP, 2-chloro-4-nitrophenyl; HSAmy, human salivary α-amylase; PNP, *p*-nitrophenyl; G2, maltose; G3, maltotriose; G4, maltotetraose; G5, maltopentaose; G6, maltohexaose; G7, maltoheptaose; MPD, 2-methyl-2,4-pentanediol.

Introduction

α–Amylases (α-1,4-glucan-4-glucanohydrolases, EC 3.2.1.1) are ubiquitous enzymes that catalyze the hydrolysis of internal α-1,4-glucosidic bonds in starch and related polysaccharides. They belong to the glycoside hydrolase family 13 (MACGREGOR et al., 2001), one of the largest families of enzymes whose members are widespread in all three domains of life. In humans, α-amylase is present in both salivary and pancreatic secretions; the overall primary structures of the pancreatic and salivary α-amylases are highly homologous, and exhibit a high level of structural similarity (BRAYER et al., 1995; RAMASUBBU et al., 1996). Human salivary α-amylase (HSAmy) is an important enzyme in the oral cavity carrying out several functions (SCANNAPIECO et al., 1995). HSAmy is monomeric, calcium binding protein with a single polypeptide chain of 496 amino acids (RAMASUBBU et al., 1996). The structure of HSAmy consists of three domains: domain A (residues 1-99, 170-404), domain B (residues 100-169) and domain C (residues 405-496). The domain A adopts a $(\beta/\alpha)_8$ barrel structure bearing three catalytic residues Asp197, Glu233 and Asp300. The domain B occurs as an excursion from domain A and contains one calcium-binding site. Domain C forms an all β-structure and seems to be an independent domain with as yet unknown function (RAMASUBBU et al., 1996). The molecular structure adapted by HSAmy is similar to the other mammalian α-amylases including the human pancreatic α-amylase with which it shares a very high degree of sequence identity ($\sim$ 97%).

The active site of HSAmy has been deduced from the structure of HSAmy complexed with pseudosaccharide derived from acarbose, a modified oligosaccharide inhibitor of amylase (RAMASUBBU et al., 2003). The

* Corresponding author

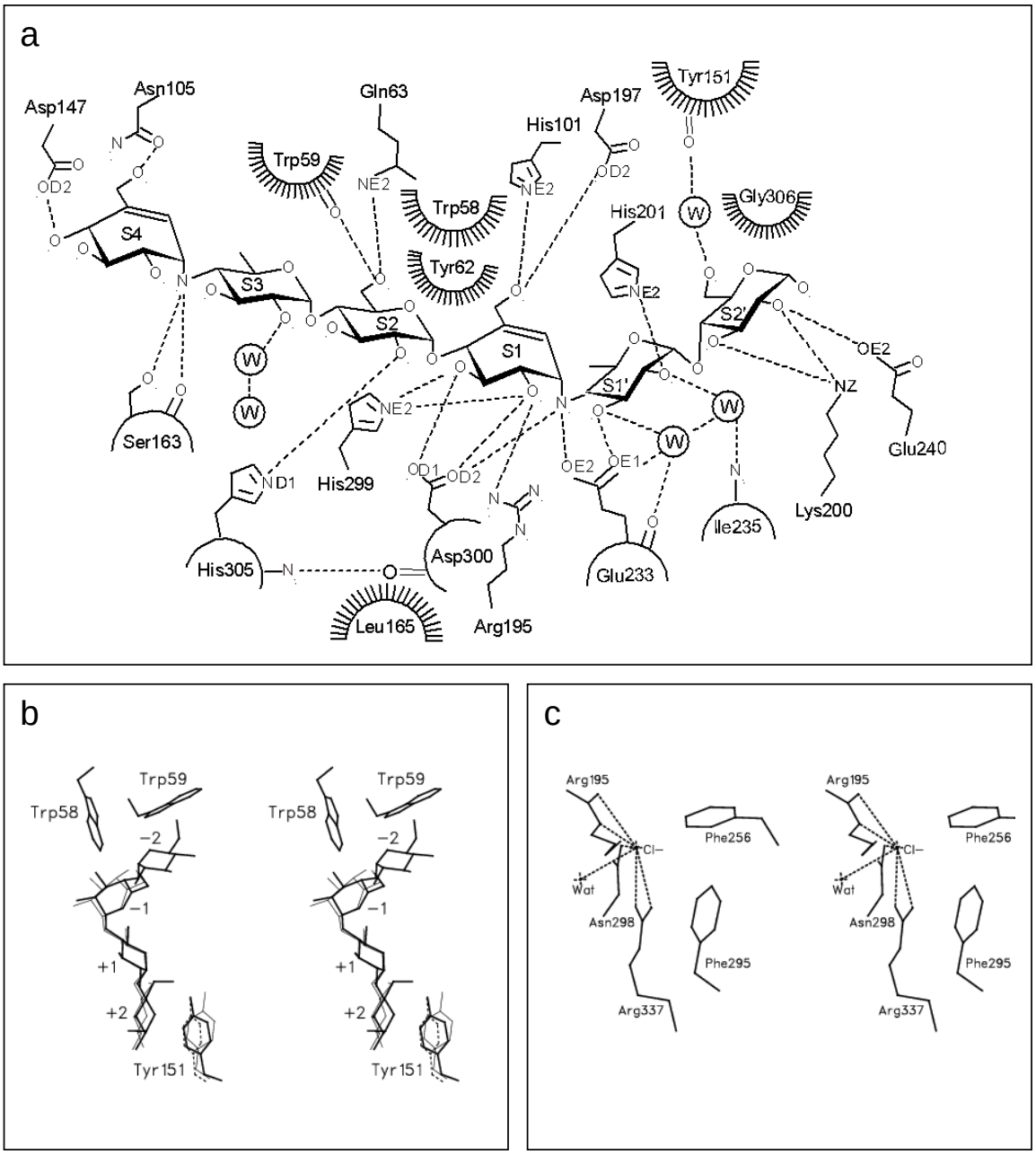

Fig. 1. Subsite architecture in HSAmy. (a) Schematic showing the substrate binding site in HSAmy. The six tandem subsites −4 through +2 are numbered according to accepted nomenclature (Davies et al., 1997). The various protein atoms and their interactions with the bound pseudooligosaccharide derived from acarbose are also shown. The hydrogen bonds are shown as dashed lines whereas the hydrophobic/stacking interactions are shown by arcs with radiating lines. Note that the binding site contains several aromatic residues especially at subsites +2, −2, and −3. (b) Sequence homology at subsite +2 of α-amylases. Comparison of sequences around subsite +2 reveals that a Tyr residue is conserved at this subsite. This residue is involved in a typical stacking interaction with bound glucose moiety. Structural conservation is shown with Tyr residues from HSAmy (thick; 1MFV), psychrophilic enzyme (thin; 1G9B) and TAKA-amylase (dashed; 7TAA) in close proximity to the subsite +2 moiety. (c) The coordination sphere around the chloride ion in HSAmy showing the clear separation of hydrophilic and hydrophobic surroundings. Two Phe residues (Phe256 and Phe 295) are dominant at the hydrophobic side.

schematic of the active site, which possesses six tandem subsites is shown in Figure 1a. The active site of HSAmy is divided into glycone binding subsites (−4, −3, −2, and −1) and aglycone binding subsites (+1 and +2) (Kandra et al., 2002; 2003; Ramasubbu et al., 2003) following the currently accepted nomenclature (Davies et al., 1997). A comparison of the active site of HSAmy with representative examples of other α-amylases (PDB code 7TAA, TAKA-amylase; 1SMD, human salivary α-amylase; and 1G9H, a psychrophilic α-amylase) reveals that subsites −1 and +1 are highly conserved with respect to the amino acid residues surrounding them. Interestingly, while the Tyr residue (Tyr151 in HSAmy) near the subsite +2 at the

reducing end is well conserved with respect to sequence and structure (Fig. 1b); residues at the subsites −2 and −3 are not. In general, aromatic amino acid residues surround these subsites; a Tyr residue at subsite +2 and Trp at subistes −2/−3 at the non-reducing end.

In addition, two aromatic residues, Phe256 and Phe295, occur in the vicinity of chloride binding site in HSAmy and other α-amylases (Fig. 1c). Several α-amylases, including HSAmy and the bacterial enzyme from *Alteromonas haloplanctis* (Feller et al., 1994) have been shown to require chloride for full catalytic activity. Recent structural determinations have shown that, in these chloride-dependent α-amylases, there is a conserved chloride ion binding site located in domain A consisting of three residues, Arg195, Asn298, and Arg337 (sometimes lysine) (Numao et al., 2002). The conservation of the residues that coordinate to chloride ion in non-chloride dependent enzymes does not come as too much of a surprise since Arg195 and Asn298 interact with catalytic residues. In contrast, Phe256 and Phe295 are conserved only within the chloride-dependent α-amylases. Herein, we report on the roles of these aromatic amino acid residues in the enzymatic activity of human salivary α-amylase through kinetic and crystallographic analysis.

Material and methods

Expression and purification of recombinant proteins

The expression and purification of the recombinant proteins was carried out using a Bac-To-Bac Baculovirus Expression System as outlined previously (Mishra et al., 2002; Ragunath et al., 2002). The mutants targeting the sites 151 and 58 were generated as described earlier (Mishra et al., 2002; Ramasubbu et al., 2004). Approximately 5 mg of purified proteins were obtained per liter of the culture.

Preparation of chloride free enzymes

Chloride free enzyme was prepared by extensive dialysis against 25 mM HEPES Buffer (pH 7.0) as suggested previously (Feller et al., 1996). Chloride activation experiments were done using 25 mM HEPES buffer with varying concentrations of NaCl (0 to 70 mM).

Enzyme activity assays

Dinitrosalicylic acid assay was used for measuring the starch-hydrolyzing activity of HSAmy and mutants at 25 °C for 3 min in 20 mM phosphate buffer (pH 6.9) containing 6 mM NaCl using 1% soluble starch as substrate (Bernfeld, 1955). Kinetic measurements were carried out using 4-nitrophenyl-α-D-maltoheptaoside (G7-PNP; Boehringer Manneheim) and *p*-nitrophenyl-α-D-maltopentaoside (G5-PNP; Sigma) in a coupled assay with 20 U/mL of yeast α-glucosidase (Boehringer Mannheim). Hydrolysis of maltooligosaccharides and maltooligosaccharide glycosides were carried out as previously described (Mishra et al., 2002; Kandra et al., 2003; Remenyik et al., 2003; Ramasubbu et al., 2004).

Structure determination of Y151M acarbose complex

Crystals of the mutant Y151M were grown using conditions previously described (Ramasubbu et al., 1991; 1996) using a protein concentration of 18 mg/mL. Diffraction quality crystals appeared over a period of one to four weeks. To obtain the complexes with acarbose, these crystals were soaked with acarbose (1 mM final concentration) in 40% MPD for 24 h and the soaked crystal was used for data collection. The crystals were mounted on loops (Hampton Research) and flash frozen to −170 °C in liquid nitrogen. Diffraction data were collected using synchrotron radiation at the CHESS beam line F-1 at liquid nitrogen temperatures using ADSC Quantum 4 CCD detector. A total of 100 frames were collected with an exposure time of one minute and an oscillation interval of 1° to give a 90% complete data set to 1.6 Å. Intensity data were integrated, scaled and reduced to structure factor amplitudes using HKL suite of programs (Otwinowski & Minor, 1997). The unit cell parameters were found to be isomorphous with those of the wild type HSAmy (Ragunath et al., 2002).

Refinement of the mutant structure (Y151M) was carried out using the CNS package (Brunger et al., 1998) wherein cycles of rigid body refinement, simulated annealing, positional and thermal B factor refinements were carried out using the coordinates of the native enzyme (PDB code 1SMD). Bulk solvent corrections were incorporated in the refinement protocols. A test set consisting of 5% of reflections was used to monitor the R_{free} behavior. Manual model rebuilding was carried out using TOM-FRODO (Jones, 1985) and O ((Jones et al., 1991). The complete polypeptide chain of the mutants were examined with Fo-Fc, 2Fo-Fc and omit maps. During this process, the mutant structure clearly showed absence of side chain density for tyrosine but showed the density for the methionine side chain. The residue at position 151 was changed to reflect the mutation and for the remainder of the refinement this residue was treated as such.

At this stage, clear-cut continuous density corresponding to the oligosaccharide ligand was observed in the active site region at subsites −2, −1, and +1. However, no oligosaccharide atoms were included in the refinement until the refinement of the protein reached convergence. The identity of the sugar moieties (either 5-hydroxymethylchonduritol or 4-amino-4,6-dideoxy-α-D-glucose or glucose) was deduced from the presence or absence density for the hydroxyl group of the side chain at position C5 in the ring (Ramasubbu et al., 2003). Additionally, difference density maps calculated by giving zero occupancy to the O6 atoms were used to assist in the identifications. The refinement was continued by the inclusion of the sugar atoms. Further examination of the density maps revealed no additional binding sites in the complex.

The final rounds of refinement were carried out using maximum likelihood method as implemented in REFMAC-5 of the CCP4 package (CCP4, 1994). Solvent molecules were added using the arp/warp procedure (Lamzin & Wilson, 1993) in the CCP4 package. The validity of the water molecules were assessed based on the following criteria: (1) the presence of a peak at least 3σ in the difference map with at least one hydrogen bond to a protein atom (N or O); or (2) if the located water molecule were part of a water chain connecting protein atoms; and (3) the water refined with a thermal factor less than 50 $Å^2$. Manual fitting was interspaced between refinements as and when neces-

Table 1. Summary of diffraction data collection values and structure refinement statistics.

Parameters	Y151M/acarbose complex
Space group	$P2_12_12_1$
Cell dimensions: a,b,c (Å)	51.66 × 73.51 × 134.36
Resolution range (Å)	42.6-1.6
Total/unique No. of reflections	182551/58813
Completeness (%): overall/last shell[a]	90.7/94.3
Mean I/σI: overall/last shell	29.1/8.0
Multiplicity	3.0
R_{merge} (%) (overall/last shell)[a]	5.9/21.1
Number of protein/ solvent/other atoms	3942/338/37
Number of reflections used	58813
B factor (Å^2): protein/solvent/other	19/30/41
R-/R_{free} (%)[b]	17.3/19.2
r.m.s deviations: bonds (Å)/angles (°)	0.008/1.1

[a] Last shell: 1.66/1.60 Å.
[b] Reflections in the test set (number/%): 3140/5.0.

sary. The programs PROCHECK (Laskowski et al., 1993), CCP4 and CNS were used for model analysis of the final refined structures (Table 1). The coordinates of the complex Y151M:acarbose have been deposited in the Protein Data Bank (PDB code 1Z32). Other structures used for comparison have the following PDB codes: 1SMD (HSAmy), 1Q4N (F256W), and 1NM9 (W58A/acarbose).

Results

Several mutants of HSAmy were expressed and purified to study the role of aromatic residues using the expression system described in Material and methods. The specific activities for the hydrolysis of starch and other oligosaccharides are given in Table 2.

Aromatic residues at the chloride-binding site

The chloride-binding site in the structure of HSAmy has hydrophilic ligands (Arg195, Asn298, Arg337) and hydrophobic residues (Phe256 and Phe295) surrounding it (Ramasubbu et al., 1996). The effect of mutation of the Phe residues at positions 295 and 256 was not similar. In fact, the introduction of a bulkier tryptophan residue at 256 (F256W) resulted in drastic reduction in activity (70-fold reduction), whereas a similar mutation at 295 (F295W) resulted in only a 1.2-fold reduction. In contrast, the mutation of hydrophilic residues at positions 195 and 337 were similar. For example, although Arg195 is conserved in all α-amylases, the introduction of a Phe at 195 (R195F) resulted in only 1.7-fold reduction in activity. Similarly, introduction of Phe at position 337 (R337F) or Ala at 337 (R337A) showed only a comparable reduction (2.6-fold or 1.5-fold reduction in activity, respectively). Similar results were obtained for R337 mutants of the human pancreatic α-amylase (Numao et al., 2002). The reduction in k_{cat} value in the chloride binding site mutants ranged from 1.4 to 3.5, except for F256W, for which the k_{cat} was almost 20-fold lower (Table 2).

The chloride free HSAmy exhibited 8% of the original activity; similar reduction was observed for all chloride-ion binding-site mutants except F256W which exhibited only marginal activity (Fig. 2). The activity of the enzymes increased as the concentration of chloride was varied between 0 to 70 mM, reaching the maximum original activity. A notable exception to this was the activity shown by F256W. Even at 70 mM chloride, the activity stayed very low (Fig. 2).

Correlation of crystal structure of F256W with its activity

Several α-amylases, including HSAmy, contain a flex-

Table 2. Parameters for the hydrolysis of starch and oligosccharides.

Enzyme	Starch	Hydrolysis of G_7-PNP		
	Specific activity (U/mg of protein)	k_{cat} (s^{-1})	K_M (mM)	k_{cat}/K_M (mM^{-1} s^{-1})
HSAmy	66400	175	0.27	648
Subsite −2 (Ramasubbu et al., 2004)				
W59A	38100	111	0.26	426
W59L	34415	75	0.16	468
W58A	350	0.43	0.39	1.1
W58L	356	0.43	0.20	2.1
W58Y	434	0.80	0.31	2.6
Subsite +2 (Mishra et al., 2002)				
Y151M	17564	28	0.50	56
Chloride-binding site (this study)				
F295W	51220	120	0.27	444
F256W	900	8.5	0.06	141
R337F	43200	109	0.24	454
R337A	24800	46	0.14	343
R195F	38000	124	0.21	590

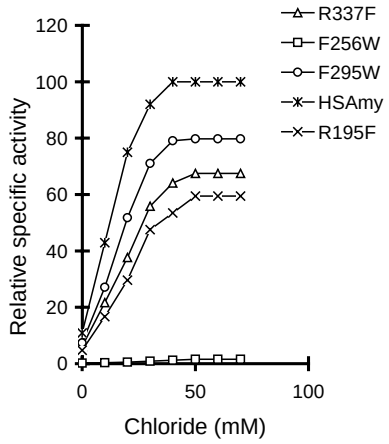

Fig. 2. Activation of HSAmy by chloride. Several mutants of HSAmy including the R195F, R337F, F256W and F295W were tested for the effect of chloride concentration. Note that the very low activity in the absence of chloride ion is restored for the mutants except F256W. Even at 70 mM chloride ion, this mutant exhibited negligible hydrolytic activity.

ible loop (residues ^{304}GHGGAG^{310}) in the vicinity of the active site. This loop becomes ordered upon substrate binding and provides stabilizing interactions at subite −2 through His305 and a water molecule (Ramasubbu et al., 2003). In addition, the atoms of this loop interact with a chain of water molecules that are positioned around the Phe256 side chain. The wild type complex (PDB code 1MFV) contains a chain of water molecules, W641, W698, W852, W668, W632 and W605, from the active site towards the bulk through the interior of the protein. This water chain is disrupted in the mutant F256W (PDB code 1Q4N) and a putative nucleophilic water molecule, (W641 in wild type) is misplaced around the catalytic residues Glu233 and Asp300 (Fig. 3). In addition, two other water molecules of the chain equivalent to W698 and W852 of the wild type are absent in the structure of the F256W. Thus, the mutation essentially altered the positioning of the water chain and as a result, altered the conformation adopted by the lower half of the flexible loop (Fig. 4b).

Aromatic residue Tyr151 at subsite +2

Previously, the kinetic analysis of mutant Y151M had shown that Y151 at subsite +2 of HSAmy takes part in substrate binding by providing a stacking interaction to the bound glucose moiety (Mishra et al., 2002). To investigate the role of Tyr151 in substrate binding, structure of a complex between Y151M and acarbose was carried out. The final refined model consists of 496 residues, 1 calcium ion and 1 chloride ion. The r.m.s. deviation as estimated from the Luzzati plot is 0.21 Å; a value is comparable to the wild type HSAmy and its mutants analyzed earlier (Ramasubbu et al., 2003; 2004). The overall structure has well-defined density at 1σ level for all the main chain and side chain atoms in the omit difference density map. The three catalytic

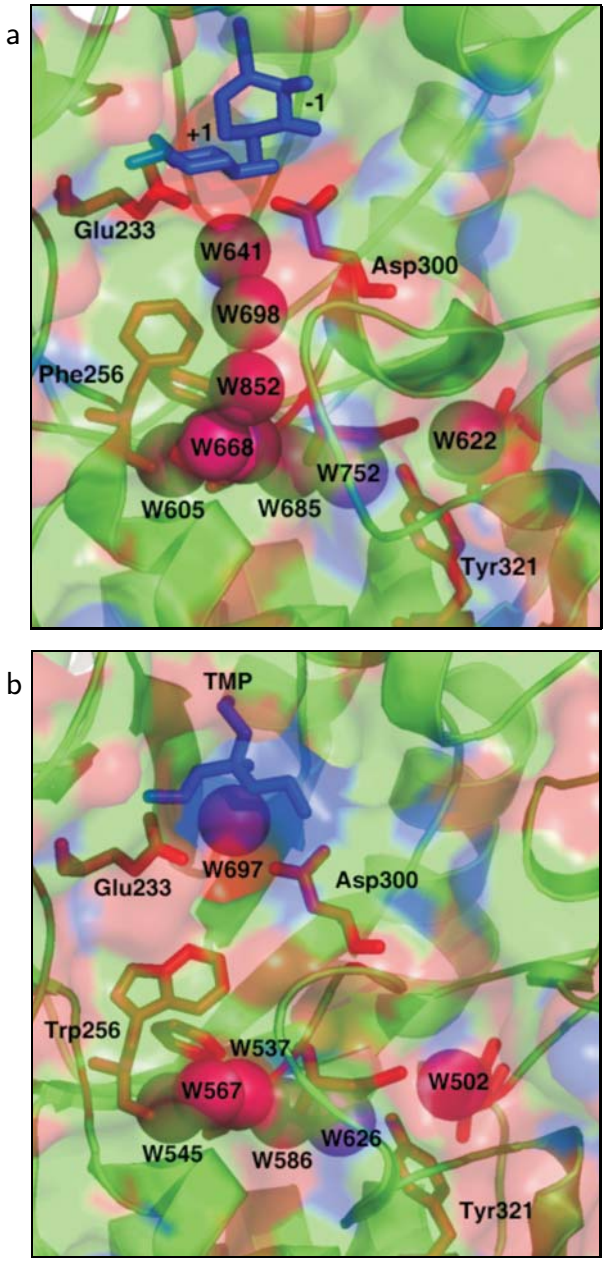

Fig. 3. Representation of the water channel in the structures of HSAmy:acarbose complex (a) and F256W:TAM complex (b). The figures were generated using PyMol (DeLano, 2002) with 50% transparency for the surface. The water chain is generally buried inside and is bordered by hydrophobic residues with some hydrogen bonding involved. Note that in the F256W:TAM complex (b), the water chain is broken around the Trp256 side chain. In HSAmy and other α-amylases, the water chain reaches the bulk solvent with suitably positioned Tyr321 (HSAmy:acarbose) or Asn331 (TAKA-amylase) residues which may act as relays.

residues, Asp197, Glu233 and Asp300 in the two structures are juxtaposed in the same way; as in the HSAmy complex with a water molecule interacting with both Glu233 and Asp300.

An important feature of the Y151M complex is that well-defined and continuous electron density, corresponding to the bound saccharide moieties, is observed

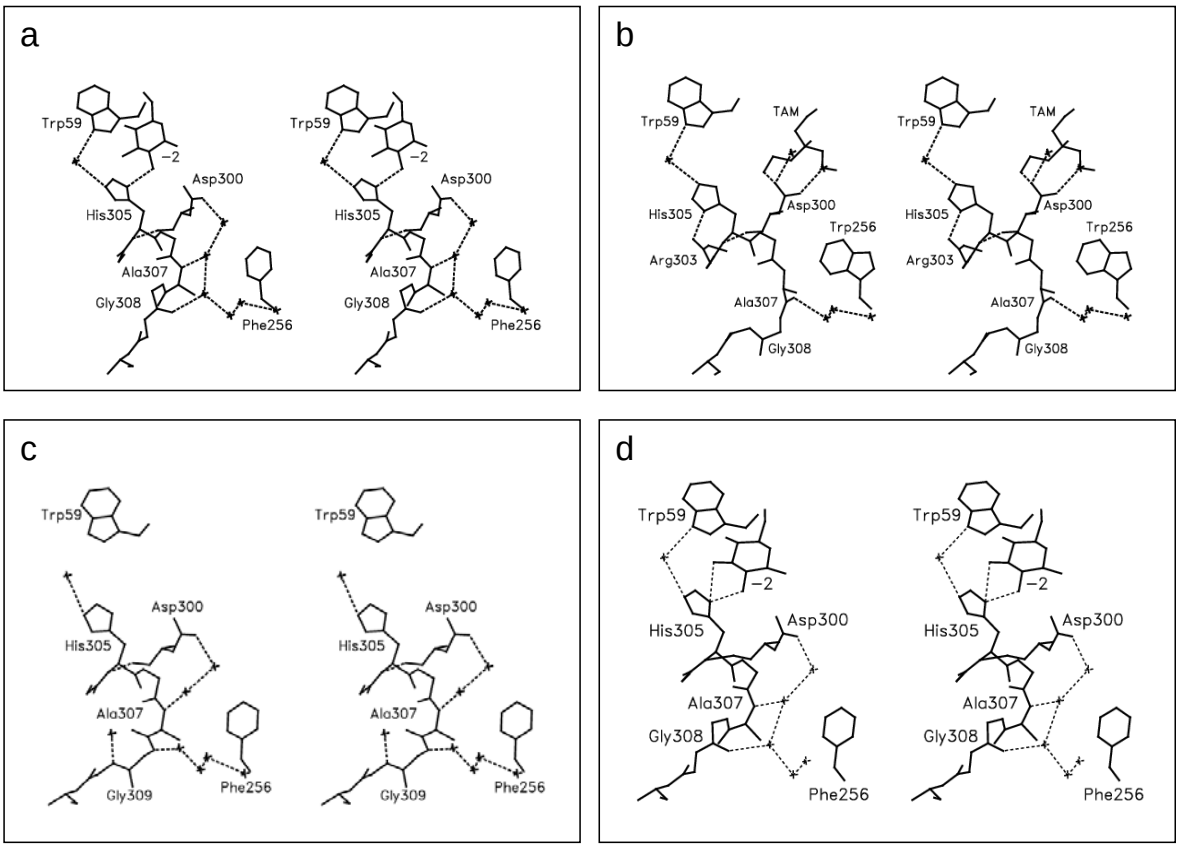

Fig. 4. Conformation of mobile loop and enzyme activity in HSAmy. Interactions involving the mobile and the water chain are shown for the structures of HSAmy (a), F256W (b), W58A (c), and Y151M (d). Not only does the mobile loop need to adopt an ordered structure, two residues Ala307 and Gly308 need to be in the proper conformation to interact with the water chain. In addition, the mobile loop His305 must be in the proper orientation to interact with Trp59, subsite −2 moiety and the catalytic residue Asp300. Note that for such interactions to occur, Gly304 and Gly309 of the mobile loop are better placed to act as anchors.

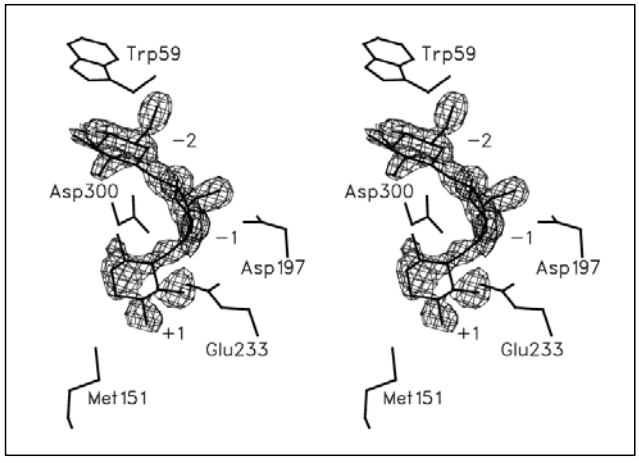

Fig. 5. Stereo drawing of the 2Fo-Fc difference density maps. The density for the bound oligosaccharide at the active site in the mutant Y151M. Note that there are only three carbohydrate moieties (GAB) that could be fitted. The identity of the residues (Glc-acarviosine) were determined using the method described earlier (Ramasubbu et al., 2003). The maps have been contoured at 1σ and the final refined coordinates of the corresponding protein or oligosaccharide residues are overlaid (shown as thick black lines).

only at subsites −2, −1 and +1 (Fig. 5). The immediate environment around the subsites −1 and +1 in Y151M complex is almost identical with that observed for the complex between HSAmy and an acarbose-derived pseudohexasaccharide (PDB code: 1MFV). The ordering of the mobile loop, upon saccharide binding in a manner reminiscent to the HSAmy:acarbose complex structure, is also observed in the Y151M complex (Fig. 4d). Other interactions involving the mobile loop (^{305}GHGAGGA^{310}) are also retained in the mutant Y151M complex. However, the ability of binding of subsite moieties at the reducing end (subsite +2) in the structure of Y151M complex is significantly different than that observed in the HSAmy complex. Analysis of the electron density at this subsite suggests only a weak binding (Fig. 5) consistent with the results obtained from kinetic studies (Mishra et al., 2002; Kandra et al., 2003). Interestingly, Met151 in the mutant adopts a side chain conformation in which the side chain lies parallel to the conformation of the tyrosine ring. In spite of this conformation being conducive for the binding of a saccharide at the subsite, electron density for the saccharide at this subsite is very weak and not fittable.

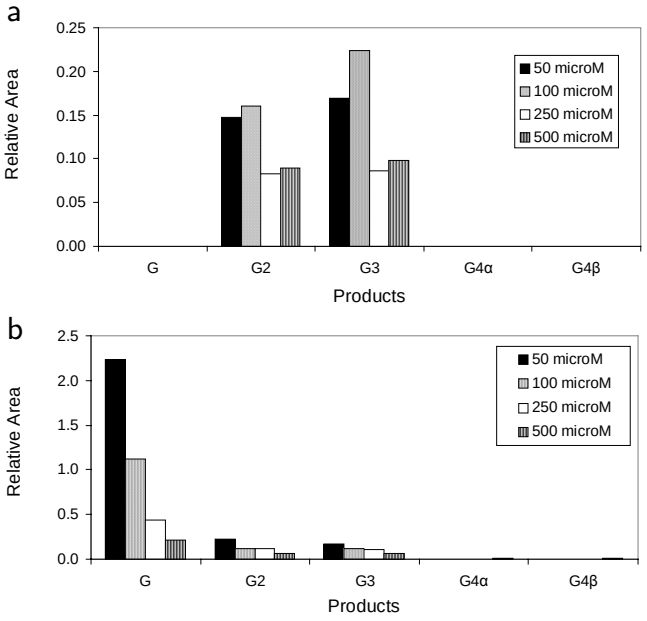

Fig. 6. Histogram showing the glucose production by HSAmy (a) and W58A (b) for the substrate G5 at various concentrations. Note that HSAmy does not produce any glucose. For W58A, glucose production is highest at lower concentration of G5 but decreases at higher substrate concentrations. Similar results were obtained for other substrates (data not shown).

Aromatic Trp residues at subsite −2

Our previous study had shown that product distribution analysis clearly showed that both W58A and W58L mutants generated more glucose than maltose (W58A>W58L>HSAmy) (Ramasubbu et al., 2004). Although more glucose was generated by G4 than G5 or G6 or G7, all of them generated more glucose than maltose. In the present study, we tested whether substrate concentration had any effect on the production of glucose and/or whether there is any selectivity in the productive-binding modes. As shown in Figure 6, lowering the G5 substrate concentration increased the amount of glucose produced. For example, there is a 2-3-fold increase in glucose production at 50 nM substrate vs. at 500 nM. The different product profiles at low and high substrate concentration reflect different binding mode affinities and rate of hydrolysis in these mutants. One possibility for these mutants to exhibit low residual activity might be due to the less specific binding mode at subsite −2. The kinetic analysis using the end-labeled maltooligosaccharides revealed that: (1) the glucose production occurred from both the reducing as well as non-reducing ends; and (2) the shorter oligosaccharides generated more glucose than longer oligosaccharides (Fig. 7a) (see also Ramasubbu et al., 2004). Similar results were obtained for the mutant Y151M as well (Fig. 7b).

Discussion

Aromatic residues and substrate binding

The hydrolysis of α-1,4-linked sugar residues by α-amylases utilizes three catalytic residues which surround two subsites: −1 and +1 (Fig. 1). The interactions around these two subsites in several α-amylases, irrespective of origin, appear to be very similar and involve the highest number of interactions with the bound substrate. However, binding at these subsites alone is not sufficient to carry out hydrolysis as evidenced by the negligible hydrolysis of maltose by these amylases. Thus, additional subsite interactions are necessary to lead to a productive binding mode. In this regard, α-amylases have a number of aromatic residues juxtaposed along the substrate-binding pocket that interact directly with the substrate. HSAmy has six tan-

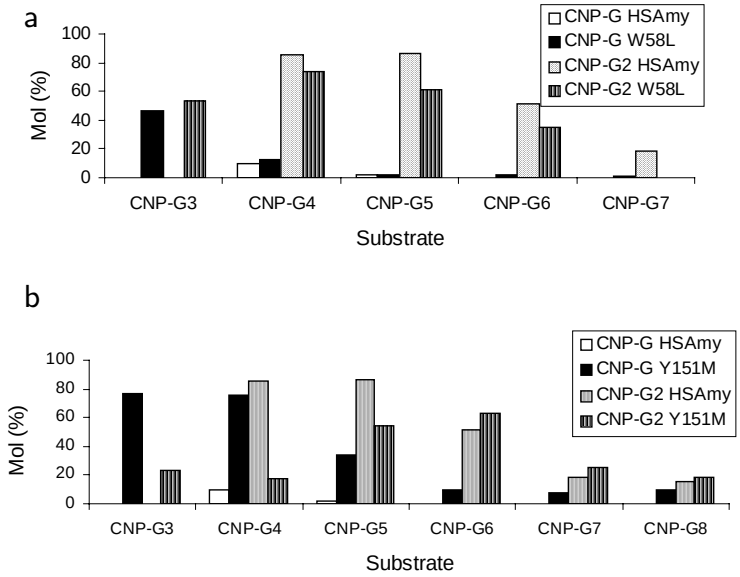

Fig. 7. Glucose production from the non-reducing end of mutants W58L and Y151M. Note that use of end-labeled substrate CNP clearly shows that glucose production occurs at the non-reducing end in both W58L (a) and Y151M (b) mutants due to changes in the productive binding modes as a result of the mutation. HSAmy, which does not cleave maltotrisaccharide and maltose, acquired the ability to cleave both G2 and G3 as a result of these mutations.

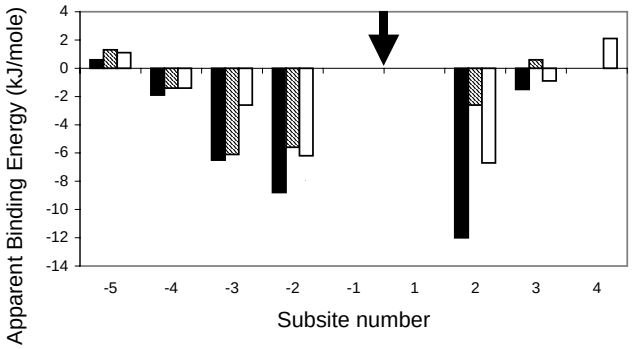

Fig. 8. Subsite maps for HSAmy (solid bar), Y151M (striped bar) and W58L (open bar). The arrow indicates the scissile bond. The reducing end of maltooligomers is situated at the right hand of the subsite map. Negative energy values indicate binding between the enzyme and aligned glucopyranosyl residues, while positive values indicate repulsion. Note the significant reduction at subsite +2 for Y151M and at subsite −3 in W58L.

dem subsites in which aromatic residues occur at both non-reducing end as well as the reducing end. The estimation of relative subsite binding energy using kinetic analysis from the hydrolysis of a series of oligomer substrates and the relative rate of formation of each product show that the apparent binding energy was higher in the immediate vicinity of subsites –1 and +1 and decreased significantly at farther subsites. The relative binding energies for HSAmy were estimated to be of the order $+2 > -2 > -3 >> +3, -4$ (Kandra et al., 2003).

Mutation of aromatic residues at these subsites reduced the binding affinity significantly (Fig. 8). Structural analysis also clearly showed that binding at these subsites is weak as evidenced by the poor electron density at these subsites (Fig. 5). This reduction in binding at these subsites has an effect in increasing the number of binding modes that would otherwise be less favorable which is reflected in the product distribution analysis (Mishra et al., 2002; Ramasubbu et al., 2003; 2004). For example, when maltopentasaccharide was used as a substrate, the wild type HSAmy produced only maltose and maltotriose. In sharp contrast, the mutants Y151M (Mishra et al., 2002) and W58L (Ramasubbu et al., 2004) generated more than two products ranging from glucose to maltotetraose. Interestingly, the Trp58 mutants exhibit the ability to hydrolyze maltose (G2) and maltotriose (G3), which the wild type enzyme HSAmy clearly lacked (Fig. 9). In the wild type enzyme, the productive binding modes in which two glucose moieties lie across the subsites −1 and +1 are overshadowed by a large number of non-productive binding modes available for G2 and G3. However, the mutation at positions 58 and 59 limits the number of non-productive binding modes and hence these mutants exhibit the ability to hydrolyze the lower oligosaccharides. As a result, a likely role for aromatics at subsites −2 and −3 might be to impart specificity in the binding of saccharides.

Aromatic residues and role in hydrolysis

One of the characteristics of α-amylases containing a flexible loop appears to be the ability for this loop to become ordered and adopting a rigid conformation. In the absence of this loop, we have shown earlier that substrate binding and catalytic efficiency in HSAmy is affected (Ramasubbu et al., 2003). The mobile loop while adopting a rigid conformation also leads to several changes in the vicinity of the catalytic site, the most notable being the mainchain-mainchain hydrogen bond interaction between Asp300 and His305. In addition to this, several other interactions occur involving the flexible loop and the water chain around the Phe256 (see Figure 4). In this regard, the aromatic residues at the non-reducing end appear to be involved in the communication between mobile loop and catalytic residue Asp300. For example, the loop conformation in the structure Y151M complex is essentially the same as that of the wild type enzyme complex whereas the conformation in the W58A complex is distinctly different. Thus, when the loop is present and ordered upon substrate binding, the interactions involving the loop can be considered to be two-fold; those involving the top half of the residues (Gly304 through Ala307) and those involving the bottom half residues (Gly308 through Gly310) with Gly304 and Gly309 acting as anchors for the movement. In HSAmy and Y151M, wherein the non-reducing end subsites are occupied, the interactions involving the top and bottom half of the mobile loop, water chain and the Trp residues are identical (Figs 4a,d). In spite of the similar interactions at the non-reducing end, the catalytic efficiency of the mutant is lower for the hydrolysis of the heptasaccharide (Table 2). Since the apparent binding affinity at subsite +2 is the highest among the various subsites (except −1 and +1; Kandra et al., 2003), binding at this subsite is significantly reduced for longer oligosaccharides. Interestingly, while many α-amylases including HSAmy do not cleave maltotriose, the mutant Y151M cleaves maltotriose entirely consistent with the reducing binding affinity at subsite +2 (Mishra et al., 2002; Kandra et al., 2003).

The introduction of a bulkier Trp residue at position 256 leads to retention of interactions between His305 and Trp59, and between His305 and Asp300, but the mobile loop itself adopts a different conformation due to disrupted water chain. Thus, the bottom half of the mobile loop does not retain all the interactions that are found in the wild type HSAmy (Fig. 4b).

In the mutant W58A complex, the inability of the loop to become ordered was evident (Ramasubbu et al., 2004) as the subsites −2 and −3 are unoccupied. Although Trp58 is not involved in substrate binding interactions, it is evidently involved in the ordering of the mobile loop, which in turn affects the catalytic efficiency. The mobile loop interactions around Trp59 are different (Fig. 4c) suggesting that the aromatic residues Trp58 and Trp59 at the subsites −2 and −3 play a critical role in enzyme activity.

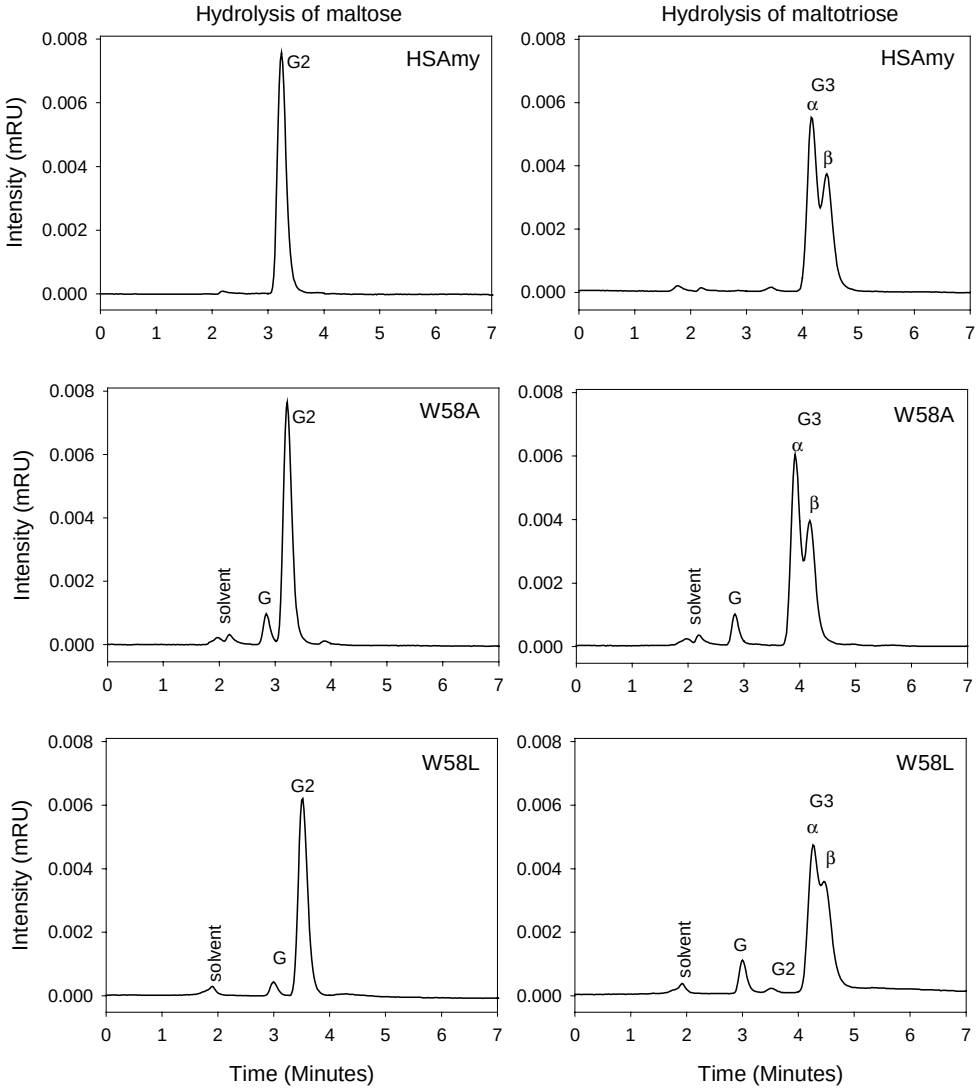

Fig. 9. HPLC analyses of the products of the reactions of HSAmy, W58A and W58L enzymes with maltose (left panel) and maltotriose (right panel). Enzyme concentration used are: HSAmy (60 nM) and mutants (500 nM). Substrate (G2 and G3) concentration is 0.5 mM. Note the peaks corresponding to G and G2 in the mutants W58A and W58L. The products were identified using standards and amylose as described in the Materials and methods section.

Aromatic residues and transglycosylation

Another interesting role of aromatic residues at the HSAmy substrate-binding site might be in controlling the transglycosylation reaction (see, Kandra et al., 2005). In the second step of the catalytic reaction, involvement of a water molecule leads to hydrolysis whereas in transglycosylation reaction another saccharide is involved. Although the mutants W58L and Y151M showed a significant reduction in its hydrolytic efficiency, both showed a remarkable increase in their transglycosidase activity (Remenyik et al., 2003; Ramasubbu et al., 2004). The structural changes with respect to the reduced substrate binding at the aglycone and glycone-binding site improved the synthetic activity of HSAmy. Recent studies have shown that *p*-nitrophenyl-glycosides are better acceptors for the mutants than for HSAmy (Remenyik et al., 2003; Ramasubbu et al., 2004). The transglycosylation activity exhibited by W58L is akin to the fungal α-amylase from *Saccharomycopsis*. This fungal α-amylase also has two highly conserved aromatic residues (Y83 and W84) located in the active center, which when mutated to Leu exhibited increased transglycosylation activity (Matsui et al., 1994).

Conclusions

We have generated several mutants of HSAmy targeting the various aromatic residues in the active site. These studies suggest a significant role for these aromatic residues. The primary role appears to be in assisting in substrate binding. In addition, the aromatic residues play a role in priming the enzyme towards hydrolysis than transglycosylation reaction. Aromatic residue at the reducing end (subsite +2) controls the size of the leaving group in a hydrolytic reaction whereas those at

the non-reducing end appear to play a role in generating communication between the mobile loop and the catalytic residue Asp300. In particular, binding at the non-reducing end subsite −2 appears to be sufficient to generate the communication between the His305 and Asp300 through the hydrogen bond interaction between the carbonyl oxygen (Asp300) and the NH of His305. These results suggest the hypothesis that aromatic residues at the active site provide a scaffold on to which the substrate positions itself first before additional stabilizing interactions occur.

Acknowledgements

This project was supported by the USPHS Grant DE12585 (NR) and by the Hungarian Scientific Research Funds T047075, T043499, T042567 (LK).

References

Bernfeld, P. 1955. Amylases, α and β. Methods Enzymol. **1:** 149–159.

Brayer, G.D., Luo, Y. & Withers, S.G. 1995. The structure of human pancreatic α-amylase at 1.8 Å resolution and comparisons with related enzymes. Protein Sci. **4:** 1730–1742.

Brunger, A.T., Adams, P.D., Clore, G.M., DeLano, W.L., Gros, P., Grosse-Kunstleve, R.W., Jiang, J.S., Kuszewski, J., Nilges, M., Pannu, N.S., Read, R.J., Rice, L.M., Simonson, T. & Warren, G.L. 1998. Crystallography & NMR system: a new software suite for macromolecular structure determination. Acta Cryst. **D54:** 905–921.

CCP4. 1994. The CCP4 Suite: Programs for Protein Crystallography. Acta Cryst. **D50:** 760–763.

Davies, G.J., Wilson, K.S. & Henrissat, B. 1997. Nomenclature for sugar-binding subsites in glycosyl hydrolases. Biochem. J. **321:** 557–559.

DeLano, W.L. 2002. Unraveling hot spots in binding interfaces: progress and challenges. Curr. Opin. Struct. Biol. **12:** 14–20.

Feller, G., Bussy, O., Houssier, C. & Gerday, C. 1996. Structural and functional aspects of chloride binding to *Alteromonas haloplanctis* α-amylase. J. Biol. Chem. **271:** 23836–23841.

Feller, G., Payan, F., Theys, F., Qian, M., Haser, R. & Gerday, C. 1994. Stability and structural analysis of α-amylase from the antarctic psychrophile *Alteromonas haloplanctis* A23. Eur. J. Biochem. **222:** 441–447.

Jones, T.A. 1985. Interactive computer graphics: FRODO. Methods Enzymol. **115:** 157–171.

Jones, T.A., Zou, J.Y., Cowan, S.W. & Kjeldgaard, M. 1991. Improved methods for building protein models in electron density maps and the location of errors in these models. Acta Cryst. **A47:** 110–119.

Kandra, L., Gyemant, G. & Liptak, A. 2002. Action pattern of α-amylases on modified maltooligosaccharides. Biologia, Bratislava **57 (Suppl. 11):** 171–180.

Kandra, L., Gyemant, G., Remenyik, J., Ragunath, C. & Ramasubbu, N. 2003. Subsite mapping of human salivary α-amylase and the mutant Y151M. FEBS Lett. **544:** 194–198.

Kandra, L., Gyemant, G., Remenyik, J., Ragunath, C. & Ramasubbu, N. 2005. Transglycosylations catalysed by Y151M mutant of human salivary α-amylase (HSA). Biologia, Bratislava **60 (Suppl. 16):** 57–64.

Lamzin, V. S. & Wilson, K.S. 1993. Automated refinement of protein models. Acta Cryst. **D49:** 129–149.

Laskowski, R.A., MacArthur, M.W., Moss, D.S. & Thornton, J.M. 1993. PROCHECK: a program to check the stereochemical quality of protein structures. J. Appl. Cryst. **26:** 283–291.

MacGregor, E.A., Janecek, S. & Svensson, B. 2001. Relationship of sequence and structure to specificity in the α-amylase family of enzymes. Biochim. Biophys. Acta. **1546:** 1–20.

Matsui, I., Yoneda, S., Ishikawa, K., Miyairi, S., Fukui, S., Umeyama, H. & Honda, K. 1994. Roles of the aromatic residues conserved in the active center of *Saccharomycopsis* α-amylase for transglycosylation and hydrolysis activity. Biochemistry **33:** 451–458.

Mishra, P.J., Ragunath, C. & Ramasubbu, N. 2002. The mechanism of salivary amylase hydrolysis: role of residues at subsite S2'. Biochem. Biophys. Res. Commun. **292:** 468–473.

Numao, S., Maurus, R., Sidhu, G., Wang, Y., Overall, C.M., Brayer, G.D. & Withers, S.G. 2002. Probing the role of the chloride ion in the mechanism of human pancreatic α-amylase. Biochemistry **41:** 215–225.

Otwinowski, Z. & Minor, W. 1997. Processing of X-ray crystallographic data in oscillation mode. Methods Enzymol. **276:** 307–326.

Ragunath, C., Sundar, K. & Ramasubbu, N. 2002. Expression, characterization, and biochemical properties of recombinant human salivary amylase. Protein Expr. Purif. **24:** 202–211.

Ramasubbu, N., Bhandary, K.K., Scannapieco, F.A. & Levine, M.J. 1991. Crystallization and preliminary X-ray diffraction studies of human salivary α-amylase. Proteins **11:** 230–232.

Ramasubbu, N., Paloth, V., Luo, Y., Brayer, G.D. & Levine, M.J. 1996. Structure of human salivary α-amylase at 1.6 Å resolution: implications for its role in the oral cavity. Acta Cryst. **D52:** 435–446.

Ramasubbu, N., Ragunath, C. & Mishra, P.J. 2003. Probing the role of a mobile loop in substrate binding and enzyme activity of human salivary amylase. J. Mol. Biol. **325:** 1061–1076.

Ramasubbu, N., Ragunath, C., Mishra, P.J., Thomas, L.M., Gyemant, G. & Kandra, L. 2004. Human salivary α-amylase Trp58 situated at subsite -2 is critical for enzyme activity. Eur. J. Biochem. **271:** 2517–2529.

Ramasubbu, N., Sundar, K., Ragunath, C. & Rafi, M. 2004. Structural studies of a Phe256Trp mutant of human salivary α-amylase: implications for the role of a conserved water molecule in enzyme activity. Arch. Biochem. Biophys. **421:** 115–124.

Remenyik, J., Ragunath, C., Ramasubbu, N., Gyemant, G., Liptak, A. & Kandra, L. 2003. Introducing transglycosylation activity into human salivary α-amylase (HSA). Org. Lett. **5:** 4895–4898.

Scannapieco, F.A., Torres, G.I. & Levine, M.J. 1995. Salivary amylase promotes adhesion of oral streptococci to hydroxyapatite. J. Dent. Res. **74:** 1360–1366.

Received November 18, 2004
Accepted March 16, 2005